

Balanced Electroabsorption Modulator for High-Linearity, Low-Noise Microwave Analog Optical Link

F. Cappelluti^{*∞}, S. Mathai^{*}, M.C. Wu^{*}, G. Ghione[∞]

^{*} Electrical Engineering Department, University of California, Los Angeles,

[∞] Dipartimento di Elettronica, Politecnico di Torino, corso Duca degli Abruzzi 24, I-10129 Torino, Italy.

ABSTRACT

The paper presents a new device for analog optical links, the balanced electroabsorption modulator, to allow the simultaneous cancellation of laser relative intensity noise, all even-order distortions, and third order intermodulation. The RF photonic link employing the new balanced modulator shows great improvement in the overall link performance with respect to conventional links using a single electroabsorption modulator. Moreover, it favorably compares with the to date highest performance links employing lithium niobate cross-coupled Mach-Zehnder modulators, proving itself an enabling technology for placement of all-semiconductor radio-frequency lightwave transmitters in high performance analog fiber optic links.

INTRODUCTION

Transmission of analog microwave and millimeter-wave (RF) signals over optical fiber is an attractive technology for use in microwave systems in view of its unique capabilities for signal processing and advantages such as low attenuation, immunity to electromagnetic interference (EMI), low weight, and small size. Successful insertion of RF photonic technologies in microwave systems hinges on the ability to meet stringent requirements in term of RF gain, noise figure (NF), and spurious free dynamic range (SFDR) [1,2]. Among intensity-modulated-direct-detection (IMDD) links, balanced RF photonic links are attractive because they can cancel the relative intensity noise (RIN) of the laser achieving shot noise limited performance. One less exploited advantage of balanced links is its ability to cancel even-order distortions. To date, the highest performance RF photonic links have employed cross-coupled LiNbO₃ Mach-Zehnder modulators (X-MZM) [3]. When the X-MZM is biased at quadrature, both RIN noise and even-order distortions are cancelled [4,5], but biasing at quadrature also produces the highest 3rd order intermodulation distortion. Therefore, RIN cancellation and large linear dynamic range cannot be achieved simultaneously.

In this paper we propose a novel device, the balanced-electroabsorption-modulator (B-EAM), for high-linearity and low-noise RF optical links. In contrast to X-MZM balanced links, the B-EAM enables the simultaneous cancellation of RIN and all even-order distortions independent of the applied bias, as well as nulling of the 3rd order intermodulation. Owing to their low voltage operation, large bandwidth, compact size, and potential for monolithic integration with semiconductor lasers, EAMs are good alternatives to LiNbO₃ MZMs. Although monolithic electroabsorption modulated lasers (EML) have been successfully demonstrated for high-performance digital applications [6], the higher RIN and lower achievable power of semiconductor lasers compared to solid-state lasers have precluded their use in high-performance RF photonic links.

THE BALANCED ELECTROABSORPTION MODULATED LINK

As shown in fig. 1(a), our proposed B-EAM consists of a pair of EAMs fed by a common coplanar waveguide (CPW). The EAM is a pin waveguide modulator fabricated on SI-InP. To reduce the mode-mismatch between fiber and waveguide, we employ a large optical cavity structure. Currently, we are working on fabrication of the modulator.

The schematic of the analog fiber link employing the B-EAM is shown in Fig. 1(b). The laser light is equally split between two EAM's. Differential modulation is achieved by feeding the RF signals to the common electrode between the EAM's. The outputs from the two EAM's are 180° out-of-phase and have equal DC intensities for all bias voltages. Since the balanced receiver detects the difference photocurrent, given by

$$I_{\text{ph}} = \frac{1}{2} \eta_{\text{D}} P_0 \left[T \left(\frac{V_{\text{DC}}}{2} + v_{\text{RF}} \right) - T \left(\frac{V_{\text{DC}}}{2} - v_{\text{RF}} \right) \right] \quad (1)$$

the RF signals from the two photodiodes add in phase, while all the even-order distortions and common mode noises are cancelled [7]. In eq. 1, η_{D} is the photodetector responsivity, $P_0 = P_{\text{L}} G_{\text{SOA}} K_{\text{PL}}$ is the output optical power from the B-EAM at zero bias, P_{L} is laser power, G_{SOA} is the semiconductor optical amplifier (SOA) gain, K_{PL} the total link loss (including insertion loss of each EAM), $T(V)$ the modulators' normalized transfer function, and V_{DC} and v_{RF} the applied DC bias and RF signal respectively.

Due to the high non-linearity of the EAM transfer curve, the SFDR is a function of the DC bias voltage. Fig. 2 shows the calculated SFDR, due to second, third, and fifth order intermodulation versus DC bias for conventional EAM and B-EAM links. Under the assumption of small signal operation, harmonic distortions and intermodulation products are calculated using a Taylor representation of the modulator's transfer function including all terms up to the fifth order [8]. To determine the output noise floor, thermal, shot, RIN noises, and the extra intensity noise introduced by the amplified spontaneous emission (ASE) from the SOA have been taken into account. RIN and ASE noise contributions, being from the same source, are cancelled at the balanced receiver, while shot noise and thermal noises generated by the modulator driving circuit and the receiver still remain factors in the total noise output power. The individual distortions can be nulled by properly choosing the bias voltage for the EAM. Except for the EAM recently proposed in [9], in conventional EAMs the nulling voltage for each distortion term is different (see Fig 2(a)), making it difficult to achieve large broadband SFDR. Conventional EAMs are usually biased at the second-order null for multi-octave applications, and at the third order null for sub-octave applications. In contrast, as shown in Fig. 2(b), the second harmonic distortion in the B-EAM link can be greatly suppressed for all bias voltages. Therefore, the bias voltage on the B-EAM can be used to null the third order derivative of the modulator transfer function. Thus, the leading distortion term becomes the 5th order intermodulation. The required stability of the modulator bias point can be achieved by tracking the photocurrent from the modulator [10].

In order to compare the proposed B-EAM link to the X-MZM link, we define an equivalent V_π for the EAM by equating the RF gain of each modulator at the intended operating bias point, 3rd order null and quadrature respectively. The small signal gain of the link is related to the first derivative of the modulator's transfer function:

$$G_{\text{RF}} = \left(\eta_D P_0 \left. \frac{\partial T}{\partial V} \right|_{V=V_{\text{dc}}} R_L \right)^2 \quad (2)$$

where R_L is the load (source) impedance. In our simulation we have used a V_π of 0.76 V. The other link parameters are $P_L = 1$ mW, $\text{RIN} = -140$ dBc/Hz, $K_{\text{PL}} = -10$ dB, and $\eta_D = 0.7$ A/W. The modulators and photodetectors are assumed to be impedance matched to the source and load impedance of $R_L = 50 \Omega$. The SOA has $G_{\text{SOA}} = 20$ dB, $\text{NF} = 10$ dB, and an optical bandwidth of 2nm. The RF link gain, with the EAM biased at the 3rd order null, is calculated to be 3.25dB, the total detected photocurrent is about 2mA.

RESULTS AND DISCUSSION

In this section simulation results are reported concerning RF link employing single EAM, B-EAM, and X-MZM. Fig. 3 shows the effect of RIN noise suppression on the link performance of B-EAM links. Using B-EAM, both NF and SFDR are not degraded by RIN noise, and shot-noise limited performance can be achieved even in the presence of RIN as high as -130 dBc/Hz. Our simulation shows that a multi-octave SFDR of 128dB-Hz^{4/5} and a NF of 8dB can be achieved with a detected photocurrent of 2mA, in contrast to the multi-octave 94 dB-Hz^{2/3}, the sub-octave 115 dB-Hz^{4/5} and NF of 24dB for the single-EAM link. As shown in Fig. 5, B-EAM link performance can be further improved by increasing the optical power, whereas, in the single-EAM link, RIN rapidly starts to dominate saturating the achievable SFDR and NF.

In Fig. 4, the NF and SFDR for the X-MZM link are also reported. Both X-MZM and B-EAM links asymptotically approach 0dB NF at high photodetected current, where they are limited by the thermal noise generated at the input of the link. B-EAM SFDR saturates to a higher value due to the simultaneous suppression of even-order distortions and 3rd order intermodulation distortions. A further advantage of B-EAM over LiNbO₃ X-MZM is monolithic integration with semiconductor laser sources and amplifiers. Monolithic integration of an EAM with a DFB laser and a SOA has been reported with fiber-to-fiber gain of 14 dB and modulator saturation power of 35mW [11].

The simulated performance reported so far has been for ideal balanced links. In reality, unbalanced modulation, optical fiber path length, and receiver responsivity may generate phase and amplitude mismatch between the photocurrents detected at the receiver, possibly degrading the effectiveness of the B-EAM link to cancel RIN noise as well as the even-order distortions. Fig. 5 illustrates the effect of the amplitude mismatch between the detected currents on noise suppression and on the achievable SFDR. To effectively achieve SFDR limited by the 5th order intermodulation (Fig. 5(a)), the acceptable relative current mismatch is $\pm 3.6 \times 10^{-3} \%$, for a detected photocurrent of 2mA. Balanced receivers with 0.5nA dark current have been reported by Islam, et. al. [12]. By exploiting the high sensitivity of the 2nd order distortion, mismatch compensation can be achieved by monitoring the 2nd order distortion in an active feedback circuit at the receiver and compensating by adjusting the responsivity of the arms of the balanced receiver. Unlike even-order harmonics, RIN noise suppression is not greatly affected by the mismatch as shown in Fig. 5(b). Our calculation shows that for a relative current mismatch of 1%, RIN will still be suppressed by 40 dB. As for the effect of phase mismatch on the degree of RIN cancellation, it is related to the autocorrelation of the RIN itself: the less the noise power spectrum is close to an ideal white spectrum, the higher the tolerable delay. Thus, it is suitable to work at frequency above the

RIN resonance peak. Employing a standard DFB laser externally modulated by a X-MZM at frequency higher than the resonance, more than 16 dB RIN suppression has been experimentally observed, even with a phase difference of 100° , corresponding to about 8.5mm fiber length mismatch for a 6.5 GHz signal [7].

References

- [1] C. Cox, E. Ackerman, R. Helkey, G.E. Betts, "Techniques and performance of intensity-modulation direct detection analog optical links," *IEEE Trans. Microwave Theory Tech.*, vol.45, p.1375, 1997.
- [2] N. Dagli, "Wide-Bandwidth Lasers and Modulators for RF-photonics," *IEEE Trans. Microwave Theory Tech.*, vol.47, p.1151, 1999.
- [3] K.J. Williams, R.D. Esman, "Optically amplified downconverting link with shot-noise-limited performance," *IEEE Photonics Technol. Letters*, vol.8, p.148-50, 1996.
- [4] L.T. Nichols, K.J. Williams, "Optimizing the ultrawide-band photonic links," *IEEE Trans. Microwave Theory Tech.*, vol.45, p.1348, 1997.
- [5] E.I. Ackerman, S. Wanuga, J. MacDonald, and J. Prince, "Balanced receiver external modulations fiber-optic link architecture with reduced noise figure," *MTT-S Symposium*, 1993, p.723.
- [6] A. Ramdane, F. Devaux, N. Souli, D. Delprat, and A. Ougazzaden, "Monolithic Integration of Multiple-Quantum-Well Lasers and Modulators for High-Speed Transmission," *IEEE J. of Selected Topics in Quantum Electron.*, vol.2, p.326, 1996.
- [7] M.S. Islam, T. Chau, S. Mathai, T. Itoh, M.C. Wu, D.L. Sivco, and A.Y. Cho, "Distributed balanced photodetectors for broad-band noise suppression," *IEEE Trans. Microwave Theory Tech.*, vol.47, p.1282, 1999.
- [8] G.E. Betts, L.M. Walpita, W.S.C. Chang, and R.F. Mathis, "On the linear dynamic range of integrated electrooptical modulators," *IEEE Journal of Quantum Electronics*, vol.22, p.1009, 1986.
- [9] R.B. Welstand, J.T. Zhu, W.X. Chen, A.R. Clawson, P.K.L. Yu, and S.A. Pappert, "Combined Franz-Keldysh and quantum-confined Stark effect waveguide modulator for analog signal transmission," *IEEE J. Lightwave Technol.*, vol.17, p.497, 1999.
- [10] G.L. Li, R.B. Welstand, W.X. Chen, J.T. Zhu, S.A. Pappert, C.K. Sun, Y.Z. Liu, and P.K.L. Yu, "Novel Bias Control of Electroabsorption Waveguide Modulator," *IEEE Photonics Technol. Letters*, vol.10, p.672, 1998.
- [11] F. Devaux, N. Souli, A. Ougazzaden, F. Huet, and M. Carré, "High speed tandem of MQW modulators for coded pulse generation with 14 dB fiber-t-fiber gain," *IEEE Photonics Technol. Letters*, vol.8, p.218, 1996.
- [12] M.S. Islam, T. Chau, A. Nespola, S. Mathai, A.R. Rollinger, W.R. Deal, T. Itoh, M.C. Wu, D.L. Sivco, A.Y. Cho, "Distributed Balanced Photodetectors for High-Performance RF Photonic Links," *IEEE Photonics Technol. Lett.*, vol. 11, p 457, 1999.

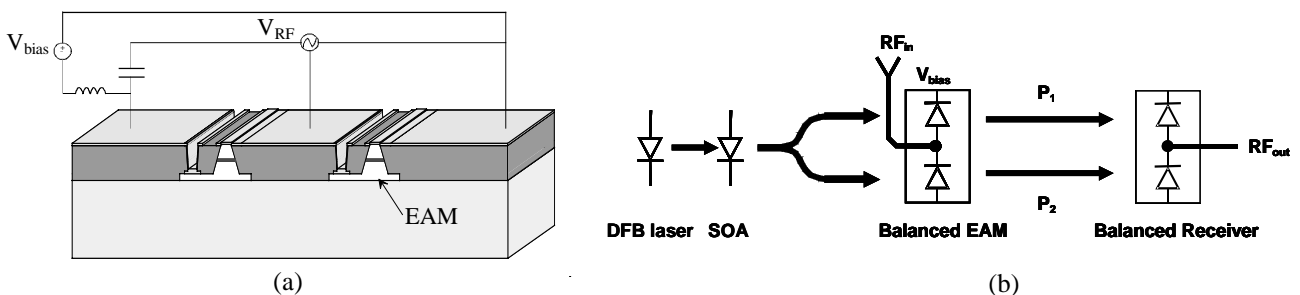


Fig. 1. (a) Schematic of the balanced EAM. (b) Schematic of the balanced-electroabsorption modulated link

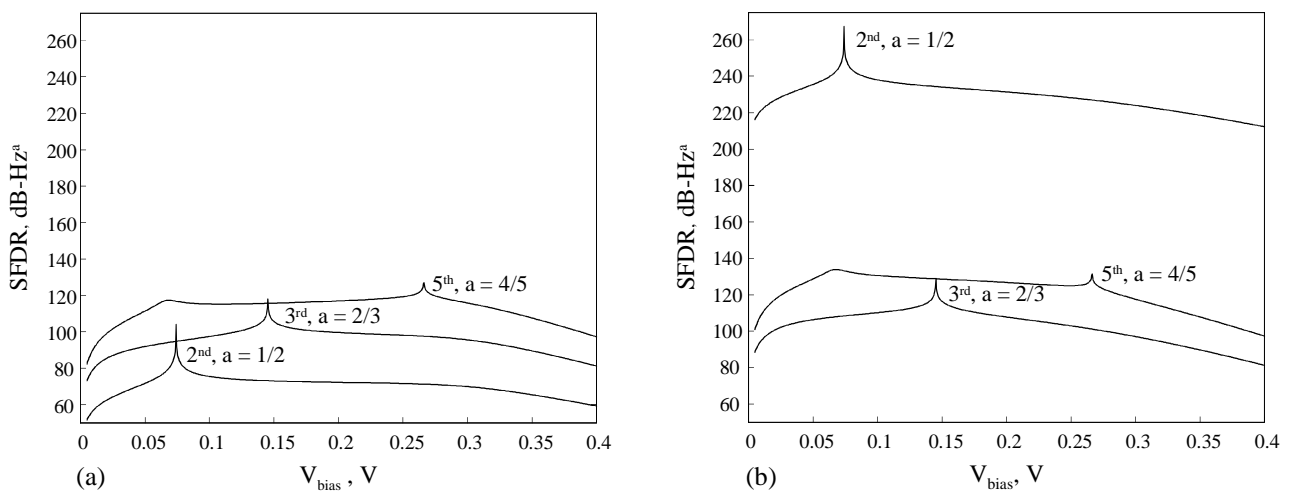


Fig. 2. Calculated SFDR for single-EAM link (a) and B-EAM link (b) for various distortions as a function of the bias voltage. In the B-EAM link the 2nd order harmonic distortion is computed assuming small mismatch between the two arms.

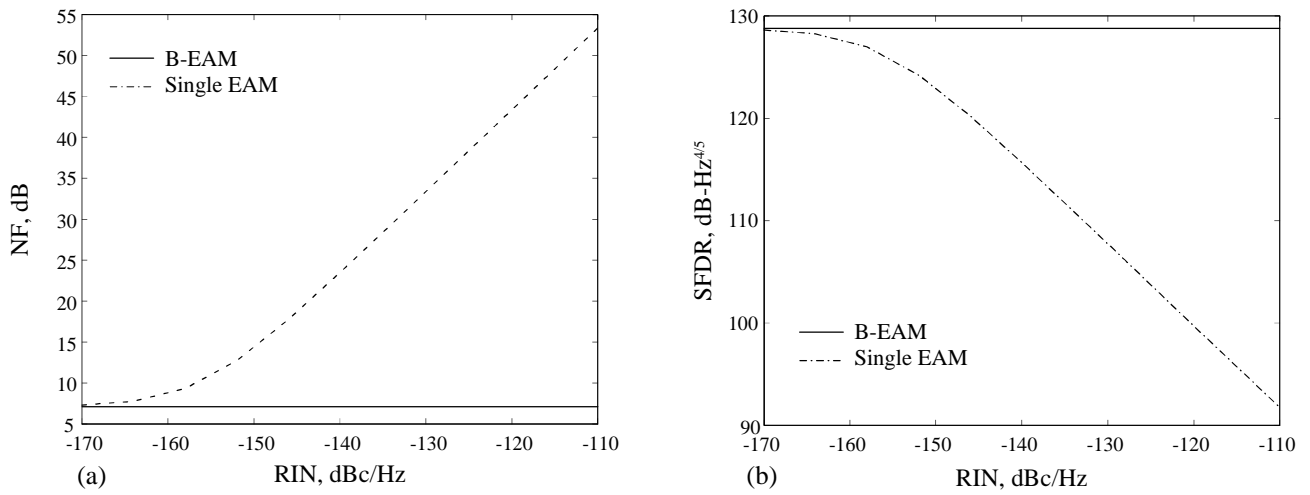


Fig. 3. Effect of laser RIN noise on NF and SFDR, for single-EAM and B-EAM link for a detected photocurrent of 2mA. The EAMs are biased at 3rd order null.

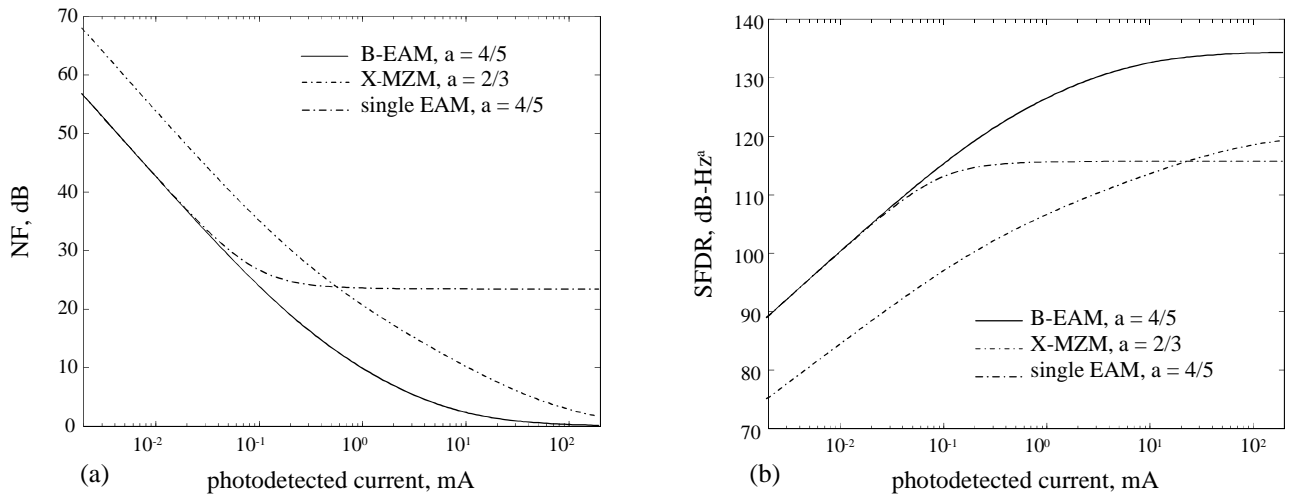


Fig. 4. NF and SFDR versus laser power for B-EAM, single EAM and X-MZM link. The EAMs are biased at 3rd order null, the X-MZM at quadrature. RIN is assumed -140 dBc/Hz.

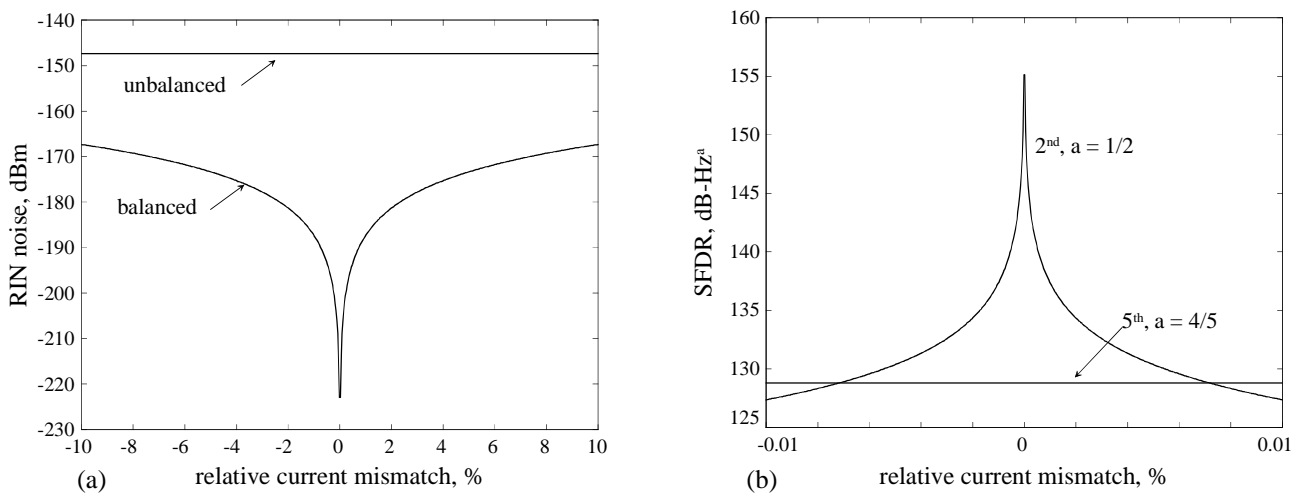


Fig. 5. Current amplitude mismatch effect on RIN noise suppression and SFDR. The noise level for the unbalanced and balanced links is computed at the same total detected photocurrent of 2mA.